

This is a peer-reviewed, accepted author manuscript of the following paper: Elobeid, M., Tao, L., Ingram, D., Pillai, A. C., Mayorga, P., & Hanssen, J. E. (2022). Hydrodynamic performance of an innovative semisubmersible platform with twin wind turbines. In ASME 2022 41st International Conference on Ocean, Offshore and Arctic Engineering: Volume 8: Ocean Renewable Energy (Proceedings of the International Conference on Offshore Mechanics and Arctic Engineering - OMAE; Vol. 8). ASME. <https://doi.org/10.1115/omae2022-79248>

HYDRODYNAMIC PERFORMANCE OF AN INNOVATIVE SEMISUBMERSIBLE PLATFORM WITH TWIN WIND TURBINES

Mujahid Elobeid*

School of Engineering, The
University of Edinburgh
Edinburgh, UK

Longbin Tao

Department of Naval
Architecture, Ocean &
Marine Engineering,
University of Strathclyde
Glasgow, UK

David Ingram

School of Engineering, The
University of Edinburgh
Edinburgh, UK

Ajit C. Pillai

College of Engineering,
Mathematics and Physical
Sciences, University of
Exeter Penryn, UK

Pedro Mayorga

EnerOcean S.L
Málaga, Spain

Jan Erik Hanssen

EnerOcean S.L
Málaga, Spain

ABSTRACT

The deployment of offshore wind turbines has focused primarily on shallow seas (such as the North Sea, Chinese coastal waters, and the New England coast) using bottom fixed foundations. However, much of the world's offshore wind resource lies in deeper waters where bottom-fixed foundations are not suitable, and floating platforms must be utilised. To date, the majority of floating concepts have been developed to support a single wind turbine. This leads to a high capital cost for each individual platform and consequently a high levelised cost of energy.

The W2Power platform (developed by EnerOcean S.L, Spain) currently supports a pair of 6 MW wind turbines on outward-leaning towers. The design significantly reduces the cost per installed MW, increases the structure's natural period, added mass, and radiation damping. The platform, patented in 2009, was the world's first twin-turbine platform and the first to be demonstrated at sea (2019).

This paper presents the hydrodynamics of a 1:40 scale model of the W2Power platform using the well-known OrcaFlex software. The analysis has been carried out under extreme and operational conditions, and the resulting hydrodynamic loads and motion response are presented.

The mooring system was found to be sensitive to wave direction, particularly when propagating along the current direction. Furthermore, the results showed advantages in the hydrodynamic responses for the W2Power platform as an innovative floating system.

Keywords: MUFOP, FOWT, semisubmersible, coupled analysis, mooring dynamics.

NOMENCLATURE

ρ_w	water density
γ	gamma
θ	theta
Lat	latitude
Lon	longitude
DoF	degree of freedom
RAO	response amplitude operator
WD	water depth
ML	mooring line
MBL	minimum breaking load

1. INTRODUCTION

Climate change is a critical issue, and wind energy is widely considered a valuable renewable energy source for decarbonising electricity generation and mitigating greenhouse gas emissions. As a result, significant effort is being made to design wind turbines that capture energy at sea. These turbines can be installed on bottom-fixed or floating foundations connected to the seabed by mooring lines. Furthermore, 80% of the offshore wind potential is in waters deeper than 60 m [1],

*Contact author: m.elobeid@ed.ac.uk

making bottom-fixed installations challenging, whereas floating installations would be feasible.

The offshore wind industry has grown tremendously in the last decade due to recent technological advances and policy encouragement worldwide. Offshore market trends indicate that floating offshore wind turbines (FOWTs) of 10-20 MW will be operational [2]. Deploying such large turbines at commercial scales using conventional single platforms is both technically challenging and, so far, has proven very expensive.

Consequently, multi-unit floating offshore platforms (MUFOPs) are being developed as viable innovations for higher installed wind capacity. Baltrop [3] highlighted the significant benefits and drawbacks of MUFOPs. Since the introduction of W2Power in 2009 [4], twin-turbine floating platforms, where two turbines use the same platform and mooring system to save installation and mooring expenses, have emerged as lower cost per MW power production systems suitable for deep-water use. Twin turbines allow more cost-efficient wind energy capture since the platform's height and loads are lower than single-turbine floaters of comparable power [5].

Such platforms are distinguished by heave plates that reduce heave and pitch motions, thereby shifting their natural frequencies towards the lower frequency region with minimum added mass and ultimately improving their hydrodynamic performance [6]. Henderson et al. [7] developed analytical tools for assessing the performance of wind farms with MUFOPs and their anticipated costs and feasible locations, particularly in the UK waters. For one specific hull shape and design configuration, the effect of columns spacing and towers inclination on the performance has been investigated by Udoh and Zou [8].

1.1 W2Power Platform

1.1.1 Development Trajectory

This paper presents the innovative W2Power twin-turbine concept currently developed by EnerOcean S.L (Spain). The platform was introduced by Pelagic Power from Norway as a novel hybrid wind-wave power concept for the offshore market in 2009. Since 2012, it has been developed primarily as a floating wind platform with multi-use capabilities (not limited to wave power). W2Power benefited from extensive preliminary research performed by Acciona Energia, NTNU and the University of Edinburgh as part of the European MARINA Platform project [9]. In the subsequent European TROPOS project (which considered multi-use platforms), it was selected as an energy-producing "satellite unit" [10].

W2Power has successfully passed five laboratory testing campaigns on a 1:100 scale model in the Curved Wave Tank at the University of Edinburgh, UK (2012–2013) and the UCC-Beaufort tank (HMRC) in Cork, Ireland (2014), and these tests have resulted in the following:

- Demonstration of concept and improvement of the platform's design.
- Appraisal of the platform's effectiveness upon two aquaculture systems
- Investigation of RAOs, moorings and forces determination of a preliminary mooring system

- Picking the appropriate wave energy converters (WECs) and their impacts on the platform dynamics, in particular, a 1:30 model of a three-WECs array and innovative control system was built and tank-tested.

Following individual validation of the key components, the Technology Readiness Level (TRL) of W2Power has been upgraded from 3 to 4.

In 2015, W2Power completed a series of validation trials at the FloWave Ocean Energy Research Facility at the University of Edinburgh. Precise sea states based on measured met-ocean conditions at EMEC, Scotland, and Cabo Silleiro, Spain, were used with a 1:40 scale model, achieving a TRL of 5.

Subsequently, W2Power has gone through several design iterations, becoming the world's first twin wind turbine platform tested at sea, achieving a TRL of 6. It should be noted that the current design omits WECs; interested readers are referred to earlier studies by Hanssen et al. [11] and Legaz et al. [12]. Figure 1 shows the 1:6 W2Power scale prototype tested in open sea near the PLOCAN platform, Canary Islands, Spain.

The current W2Power design is engineered to support a pair of original equipment manufacturers (OEMs) wind turbines on out-leaning towers, as studied here with two "generic" 6 MW turbines and giving each platform 12 MW rated power. The platform is anchored to the seabed by a single point mooring system comprising three lines.



FIGURE 1: W2POWER PLATFORM PROTOTYPE DURING 2019 SEA TESTS. PHOTO COURTESY OF ENEROCEAN.

1.1.2 Wind Farm Scale Advantages

EnerOcean has proposed two wind farms with a total capacity of 180 MW, and up to 15 floating platforms are likely to be deployed. W2Power is the most cost-effective technology at the wind farm scale in terms of cost-effectiveness [13 - 14], and provides the following:

- Maximisation of power generation due to its weathervaning system that allows the platform to align with the predominant wind direction and eliminates conventional yaw

- W2Power, with its light-weight but stable design, offers up to twice the rated capacity of a single turbine floater while using less material (saving up greater than 25% of steel weight)
- Assembling two turbines on a single platform can be done in a dry dock or a load-out quay, which keeps time and installation costs down since fewer tows and moorings are required
- A W2Power wind farm reduces inter-array cabling and mooring requirements by increasing turbines density in the array, thus improving seabed space management.

1.1.3 Model Design Description

This study considers a 1:40 scale model of the W2Power platform, which is a triangular semi-submersible structure that supports a pair of OEM wind turbines mounted on outward-leaning towers at columns A and C.

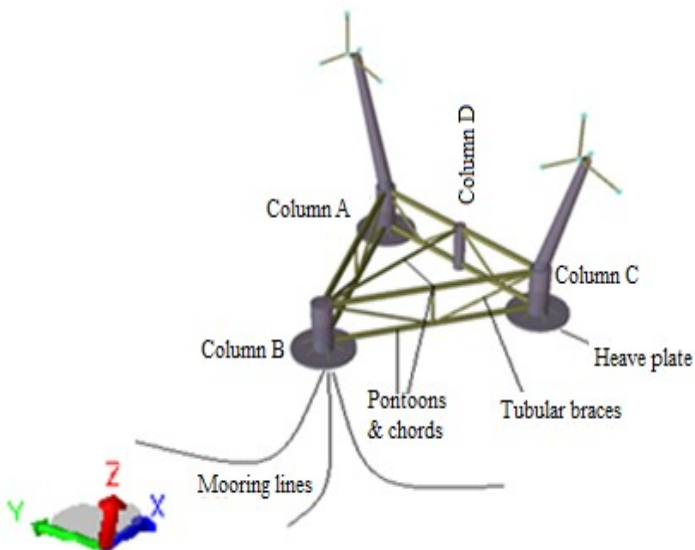


FIGURE 2: SCHEMATIC REPRESENTATION OF THE MODEL'S COMPONENTS.

TABLE 1: MAIN PARTICULARS OF THE FULL-SCALE W2POWER PLATFORM.

Description, unit	Prototype
Draft, m	15
Water depth, m	200
Outward leaning angle, °	15
Corner columns diameter, m	9
Column D diameter, m	5
Columns heights, m	25
Towers bases separation, m	90

2. ANALYSIS METHODS

The floating system here consists of two components:

- 1) the floater, modelled as a large rigid body with six DOFs
- 2) the mooring lines, modelled as slender bodies using the Morison equation

The hydrodynamic loads on these components are evaluated by employing different theories since their dimensions differ. A fully coupled analysis is used to evaluate the system's performance. The non-linear interactions between hydro- and mooring- dynamics are captured by solving the governing equations in the time domain:

$$([M] + [A])\ddot{X} + [B]\dot{X} + [C]X = F_{wave} + F_{moor} \quad (1)$$

Where, $[M]$ is the 6×6 structural mass (dry mass + inertia) matrix, which includes platform, towers, nacelles, and rotors as superstructures. $[A]$ is the 6×6 frequency-dependent added mass, B is the 6×6 potential damping matrix, and C is the 6×6 hydrostatic stiffness matrix. F_{wave} is the 6-DOF wave forces (excitation, viscous and drift forces) in which the Newman approximation was utilised to account for wave drift loads [15], and F_{moor} is the mooring force.

2.1 Numerical Model Setup

The numerical model is built at a scale of 1:40, and its properties are listed in Table 2. Then numerical simulations were performed using the SESAM (GeniE) software developed by DNV [16] and Orcina Ltd's packages (OrcaWave and OrcaFlex) [17 - 18].

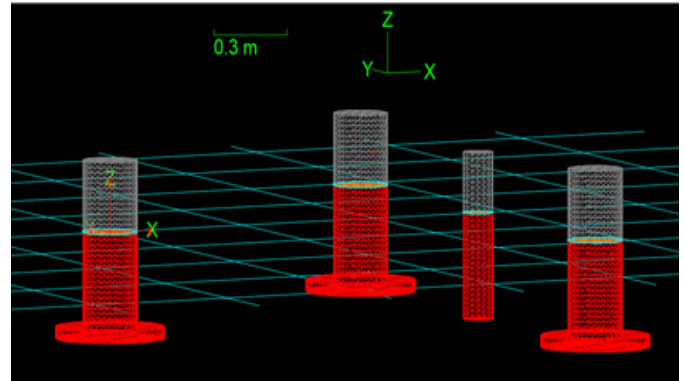


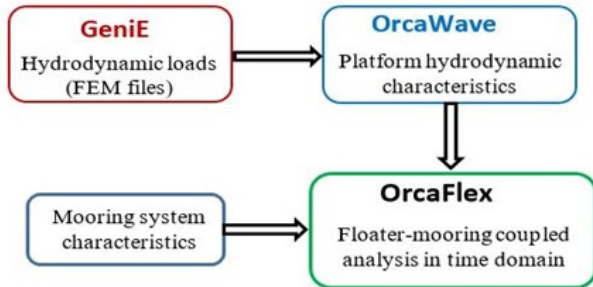
FIGURE 3: PANEL MODEL IN ORCAWAVE, WET SURFACES (IN RED) BELOW THE LOADING CONDITION.

GeniE was utilised to construct and generate FEM models of the platform's substructures: the panel model including the four columns (A, B, C, and D) and the Morison model represented by the pontoons and braces. Then OrcaWave was used to perform the hydrodynamic study based on the 3D potential theory. As a result, the hydrostatic stiffness coefficients were obtained, along with the frequency-dependent hydrodynamic added mass and damping.

TABLE 2: SCALE MODEL PROPERTIES.

Mass, kg	122.087		
Centre of mass (x, y, z), m	1.2E+00	-3.3E+05	1.9E-01
Centre of buoyancy (x, y, z), m	1.2E+00	1.6E-07	-2.3E-01
Waterplane area, m ²	1.3E-01		
Mass moments of inertia, kg.m ²	4.0E+05	6.7E-03	-4.1E+01
	6.7E-03	4.0E+05	1.9E-15
	-4.1E+01	0.0E+00	4.0E+05

After obtaining the platform's hydrodynamic characteristics (i.e. RAOs), all substructures were imported into the OrcaFlex to analyse the floater and mooring coupled system in the time domain. The coupled analysis model setup is depicted in Figure 3.


FIGURE 3: MODEL SETUP FOR COUPLED ANALYSIS.

2.2 Environmental Conditions

The environmental data considered here are for a potential deployment site off the island of Gran Canaria in the Atlantic Ocean, as shown in Figure 4. The National and Kapodistrian University of Athens provided wind and wave hindcast data from 2001 to 2010 [19].

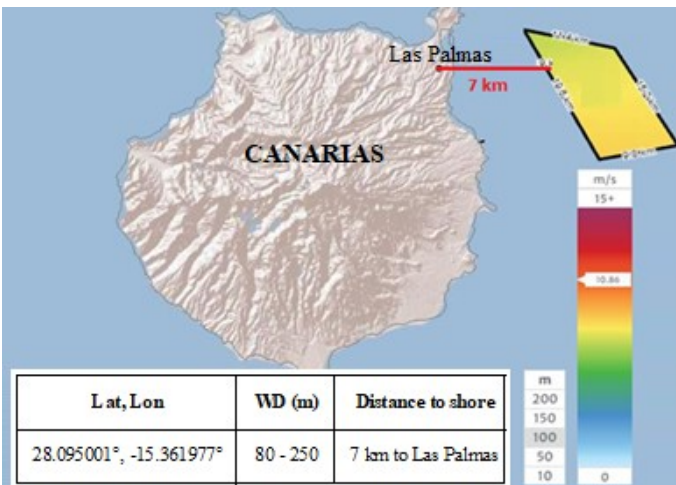
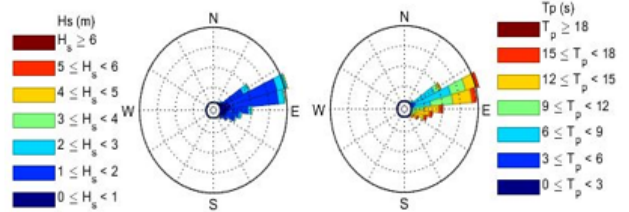

FIGURE 4: REFERENCE SITE (GLOBAL WIND ATLAS) [20].

Figure 5 shows the distribution of significant wave height (H_s) and peak wave period (T_p) by sector. As can be seen, the dominant sector is East-North-East, with the majority of long-period waves (mostly between 6 and 15s) and large significant wave height emanating from that direction.


FIGURE 5: DIRECTIONAL WAVE ROSE: (LEFT) H_s AND (RIGHT) T_p .

Accordingly, neglecting aerodynamic loads and considering both waves and current conditions, operational load cases for two wave directions are simulated, as described in Table 3.

TABLE 3: PARTICULARS FOR OPERATIONAL LOAD CASES SIMULATIONS.

Description	Full Scale	Model Scale
Water depth (m)	80	2
	200	5
Current conditions		
Speed (m/s)	1	0.158
Direction (°)	180	180
Wave conditions (JONSWAP spectrum)		
H_s (m)	1.5	0.0375
T_p (s)	8	1.265
γ	2	2
Directions (°)	180	180
	210	210

2.3 Frequency-domain Hydrodynamic Analysis

2.3.1 Eigenfrequency Analysis

Due to the floater's symmetry, pitch and roll motions are nearly identical, and the mooring system significantly influences horizontal motions. Therefore, only heave and pitch motions are of interest. When the platform is analysed without a mooring system, the restoring force is generated mainly by the large waterplane area, which remains unchanged for the two water depth conditions due to the use of the same floater, and also the body mass remains unchanged. However, only the added mass term varies in response to the dynamic pressure generated by the platform's motion.

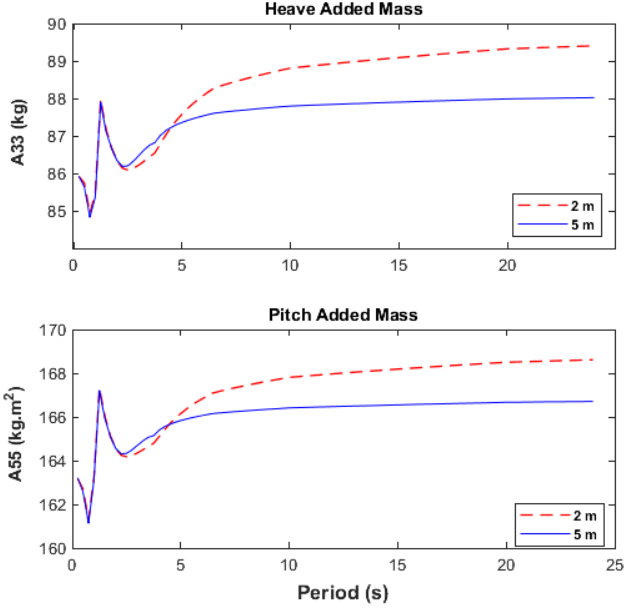


FIGURE 6: ADDED MASS OF HEAVE (A33) AND PITCH (A55) MOTIONS IN A 0° WAVE HEADING FOR WATER DEPTHS OF 5 AND 2 M.

The added mass is dependent on the period of the excitation wave and converges towards a constant value for both heave and pitch, as illustrated in Figure 6. Then the natural periods, T_{Ni} , for the heave and pitch responses can be calculated by Eq (2), and Table 4 summarises the results.

$$T_{Ni} = 2\pi \left(\frac{M + A_{ii}}{C_{ii}} \right)^{0.5} \quad (2)$$

Where, M is the body mass, A_{ii} and C_{ii} are the added mass and restoring stiffness in the i th DoF, respectively.

TABLE 4: EIGENFREQUENCY CALCULATION FOR WATER DEPTH 5 AND 2 M.

Description	DoF			
	Heave		Pitch	
Water depth (m)	5	2	5	2
Body mass (kg, kg.m ²)	122.087	122.087	180.189	180.189
Added mass (kg, kg.m ²)	87.887	89.326	166.342	167.330
Restoring (N/m, N.m)	1311.923	1311.523	2178.313	2178.313
Natural period (s)	2.514	2.523	2.506	2.510

2.3.2 Platform RAOs Motion

Figure 7 compares the response amplitude operators (RAOs) for heave and pitch motions. The RAOs reveal that the resonance occurs at a wave period of approximately 2 to 3 s, which is consistent with the eigenfrequency calculations in Table 4, especially in the heave response. Furthermore, as the water depth decreases, there is a significant rise in pitch response, particularly at low frequencies. However, this is not seen in the heave RAO; hence, more illustrations (i.e. excitation forces) might be presented that are not shown in this study. Following that, the hydrodynamic characteristics of the platform were determined for each water depth in preparation for time-domain analysis of the floater-mooring coupling.

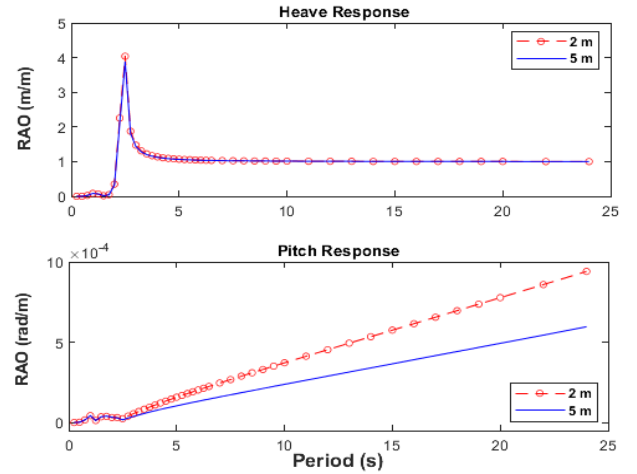


FIGURE 7: HEAVE AND PITCH RAOs IN A 0° WAVE HEADING FOR WATER DEPTHS OF 5 AND 2 M.

2.4 Time-domain Hydrodynamic Analysis

To more accurately model drag loadings on submerged parts of the hull, large members (i.e. columns and heave plates) and cross members (i.e. pontoons, chords, and tubular braces) were modelled in OrcaFlex as Morison elements. Furthermore, all columns and the three heave plates are equipped with Morison elements. In accordance with [21] and [22], the drag coefficients used in the analysis are listed in Table 5, with colour coding consistent with that in Figure 8.

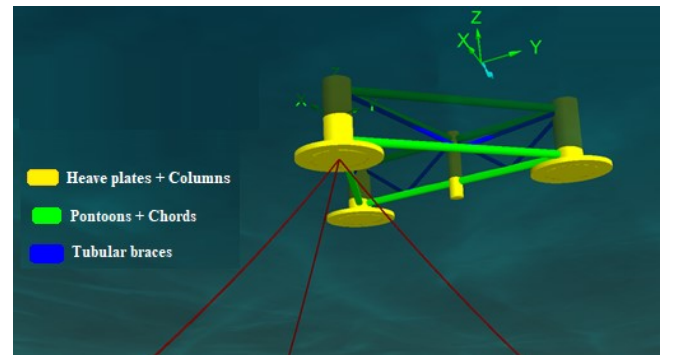


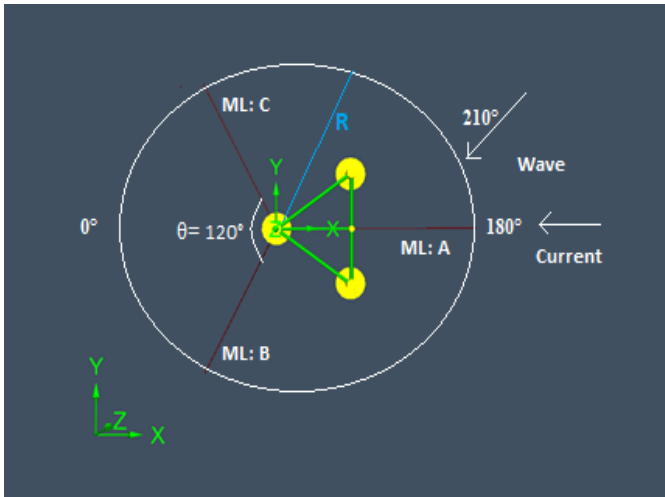
FIGURE 8: MORISON DRAG ELEMENTS RENDERING AND THEIR COLOUR CODES IN ORCAFLEX.

TABLE 5: DRAG COEFFICIENTS FOR MORISON ELEMENTS.

Hull component	Drag Coefficient (Cd)
Corner columns (A, B & C)	0.61
Middle column (D)	0.56
Heave plates	0.68 4.8 in z-direction
Pontoons and chords	1
Tubular braces	0.63

2.5 Mooring System

Three catenary lines (A, B and C) are placed symmetrically along the platform's Z-axis and spread by 120° to anchor it to the seabed, as seen in Figure 9. According to DNV guidelines [23], stud-less chains of a drag coefficient of 2.4 were selected; the characteristics of the mooring system are listed in Table 6.


FIGURE 9: TOP VIEW OF MOORING LINES ARRANGEMENT AND ENVIRONMENTAL LOADING DIRECTIONS.
TABLE 6: CHARACTERISTICS OF THE MOORING SYSTEM MODELLED.

Description, unit	Water depth	
	5 m	2 m
Line grade and type	R4 - studless chains	
Dry-line weight, N/m	3.01	
Wet-line weight, N/m	2.61	
Nominal chain diameter, mm	8.00	
Minimum breaking load (MBL), N	31.38E+03	
Axial stiffness, N	1.32E+06	
Fairlead pretension, N	33.37	11.71
Line unstretched length, m	22.93	9.17
Fairlead depth, m	0.375	0.375
Anchor radius (R), m	21.35	8.54
Anchor depth, m	5	2

2.6 System Survivability Analysis

To check the system survivability, contour surfaces for joint wind and wave parameters are constructed based on long-term joint distributions of mean wind speed at 100 m height (U_w), significant wave height (H_s) and spectral peak period (T_p), with the probability of exceeding corresponding to a 50-year return period. The contour surfaces shown in Figures 10 and 11 were produced using the ViroCon, Python-based, software [24]. The zero-crossing period (T_z) was estimated using the relationship $T_p = 1.2859 T_z$, and as recommended by DNV [22], the duration of each sea state is 3600 s. Accordingly, four extreme load cases (LCs) are defined with six different wave seeds for each and summarised in Table 7. Likewise, the load cases in Table 3 are considered to analyse the performance of the floater-mooring system under operational conditions.

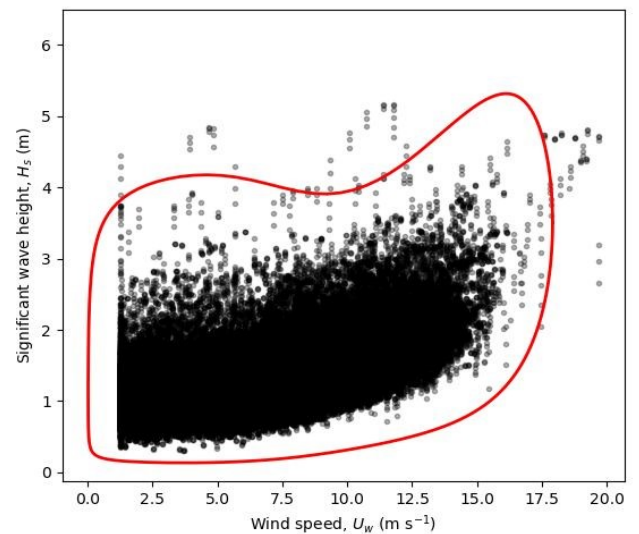
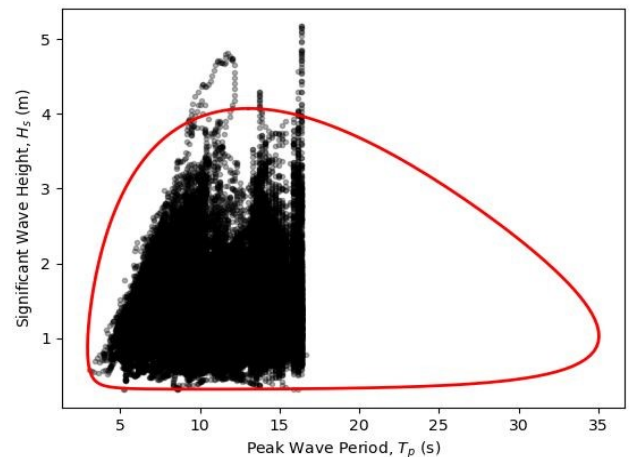

FIGURE 10: 50-YEAR ENVIRONMENTAL CONTOURS FOR U_w AND H_s .

FIGURE 11: 50-YEAR ENVIRONMENTAL CONTOURS FOR T_p AND H_s .

TABLE 7: PARTICULARS FOR SURVIVABILITY ANALYSIS.

Description	Full Scale	Model Scale	
	80	2	
Water depth (m)	200	5	
Simulation time (s)	3600		
Wave conditions (JONSWAP spectrum)			
LC 1	Hs (m)	4	0.100
	Tp (s)	16.5	2.609
LC 2	Hs (m)	4.1	0.103
	Tp (s)	13.5	2.135
LC 3	Hs (m)	3.8	0.095
	Tp (s)	8	1.265
LC 4	Hs (m)	4	0.100
	Tp (s)	10	1.581
γ	3.3		
Direction (°)	180		

2.7 Simulation Setup

Regarding the simulation settings, the platform is positioned, as seen in Figure 9. Since no wind is considered, both waves and currents propagate in the x-direction (at 180°). While the current direction remains unchanged, waves hit the floater at 210°, which leads to a 30° misalignment between the wave and current directions.

3. RESULTS AND DISCUSSION

3.1 Extreme Condition Results

The ultimate limit state (ULS) check is performed to ensure that individual mooring lines are strong enough to withstand the loads imposed by extreme environmental conditions. According to standard DNV-OS-E301 [23], the design equation in the form of a utilisation factor (UF) can be expressed as follows:

$$UF = \frac{T_d}{S_c} < 1 \quad (3)$$

$$T_d = (\gamma_{mean} * T_{mean}) + (\gamma_{dyn} * T_{dyn}) \quad (4)$$

Where, S_c is the characteristic mooring line strength and was obtained from the minimum breaking strength ($S_c = 0.95 \times S_{MBS}$). T_d is the design tension, γ_{mean} and γ_{dyn} are partial safety factors for the mooring line's mean (T_{mean}) and dynamic (T_{dyn}) tensions, respectively, which have been determined in accordance with a consequence class 1, see Table 8.

TABLE 8: PARTIAL SAFETY FACTORS FOR ULS.

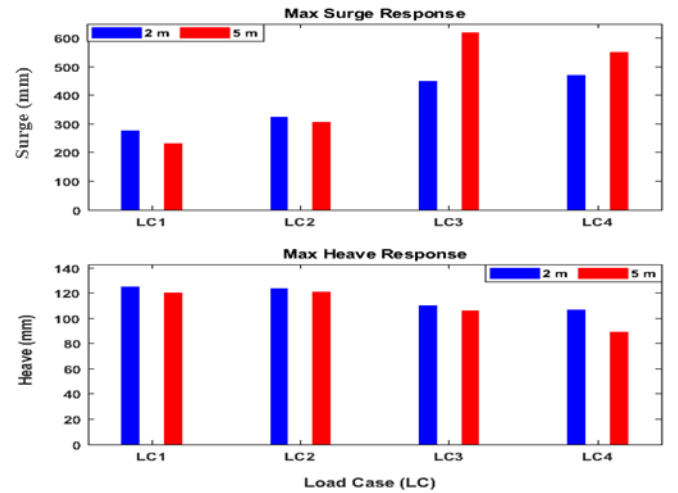
Consequence class	Safety factor for mean tension (γ_{mean})	Safety factor for dynamic tension (γ_{dyn})
1	1.10	1.50
2	1.40	2.10

Matlab was utilised for post-processing. The results of the ULS analysis are summarised in Table 9. In all loading cases, the utilisation factors for all lines were found to be quite conservative, indicating that the mooring lines are sufficiently strong to withstand the extreme waves in that location. However, mooring line A showed a higher utilisation factor than the other two lines due to its alignment with the incoming waves.

TABLE 9: ULS RESULTS FOR THE MOORING LINES.

LC	M L	T_{mean} (N)		T_{dyn} (N)		UF	
		2 m	5 m	2 m	5 m	2 m	5 m
LC1	A	13	35	14	13	1.98E-03	3.28E-03
	B	9	30	3	8	7.74E-04	2.56E-03
	C	9	30	3	8	7.71E-04	2.58E-03
LC2	A	13	35	22	29	2.75E-03	4.68E-03
	B	9	30	3	11	8.18E-04	2.78E-03
	C	9	30	3	11	8.13E-04	2.84E-03
LC3	A	18	39	204	84	1.85E-02	9.64E-03
	B	8	29	9	15	1.31E-03	3.11E-03
	C	8	29	13	20	1.60E-03	3.48E-03
LC4	A	15	37	836	68	7.25E-02	8.17E-03
	B	8	29	6	13	1.00E-03	2.90E-03
	C	8	29	11	19	1.47E-03	3.49E-03

The maximum mooring line tension and floater surge and heave movements are some of the most critical design criteria for semisubmersibles. Figure 12 illustrates the surge and heave motions of the platform under extreme conditions, whereas Figure 13 depicts the maximum tension in the three lines. As can be observed, the three parameters are controlled by the significant wave height (H_s) and peak period (T_p). The heave response reduces as the wave period decreases, whereas the surge response increases.


FIGURE 12: MAXIMUM SURGE AND HEAVE MOTIONS FOR EACH EXTREME LOAD CASE AND TWO DEPTHS.

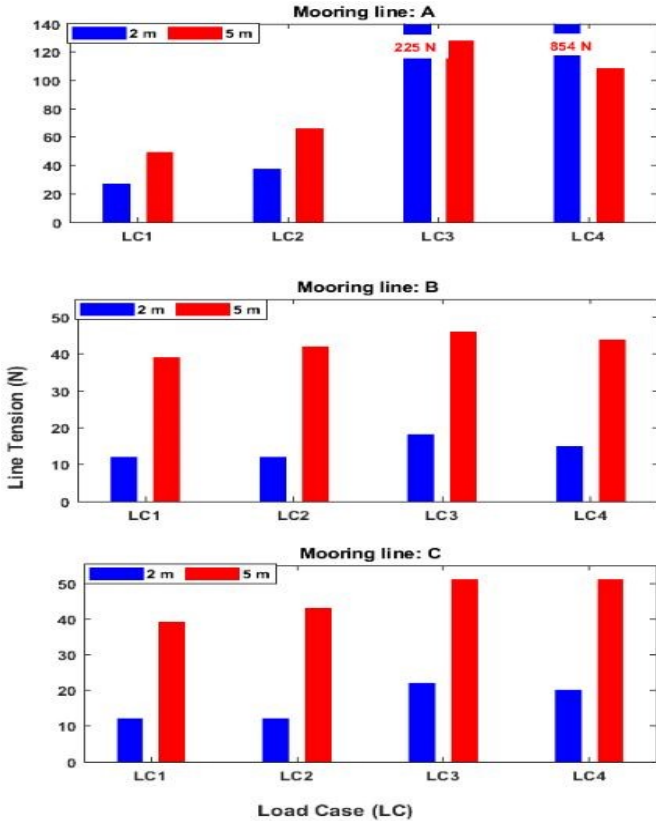


FIGURE 13: MAXIMUM MOORING LINE TENSIONS FOR EACH EXTREME LOAD CASE AND TWO DEPTHS.

At a water depth of 2 m, mooring line A experienced extremely high tensions of 225 N and 854 N during the most severe wave circumstances due to the line's direction of collinear waves and currents (180°), but these tensions are still less than the line MBL. The surge follows a similar pattern, and it is interesting to note that the maximum tension and surge do not coincide. One of these values (both $T_{\max} = 225$ N and $\text{Surge}_{\max} = 450$ mm) occurred while the wave height ($H_s = 0.095$ m) was less than the maximum, emphasising the significance of modelling different realisations (i.e. random seeds) and employing a focused-wave technique to reproduce an extreme wave condition of the sea state of interest, particularly for single mooring systems. This argument is consistent with the findings of Hann et al. [25] and Coe et al. [26], who concluded that a single focused wave was insufficient to accurately quantify the extreme loads encountered by a single taut moored wave energy converter. On the other hand, the heave response was found to have values relatively close to those observed at 5 m water depth, averaging about 0.11 m.

3.2 Operational Condition Results

3.2.1 Mooring Line Tension

This section discusses the platform's performance under the operational load case defined in Table 3. The effective tensions at the fairleads of three mooring lines are shown in Figure 14 for an operational load case and two water depths. The coexistence

of waves and currents causes the most substantial tensions in line A. The average tension at a depth of 2 m is around 12.7 N, while at a depth of 5 m, it is approximately 35 N. As can be seen, the tension at 5 m water depth is approximately 1.7 times that at 2 m. This is due to the increased tension associated with the deeper water level caused by the long line suspended and laid at the seabed.

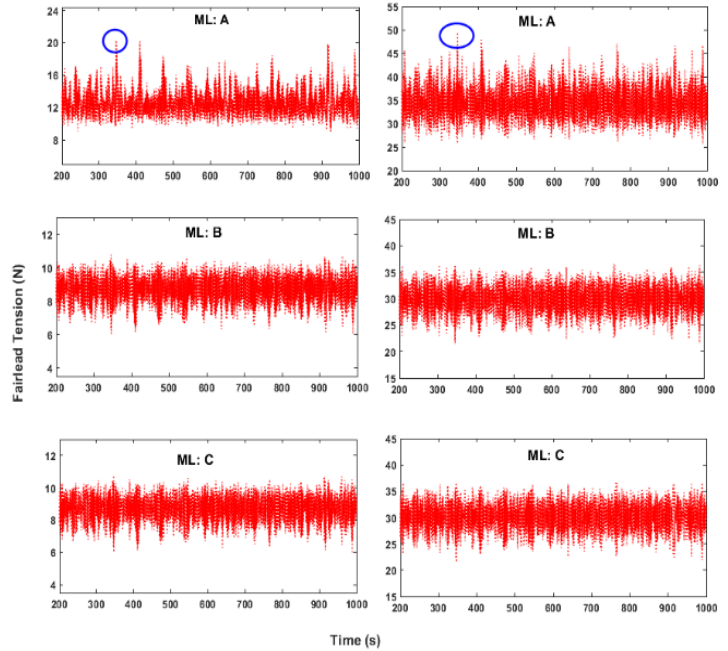


FIGURE 14: TIME-SERIES RESULTS OF THE MOORING LINES TENSION AT WAVE HEADING 180° AND WATER DEPTH 2 M (LEFT) AND 5 M (RIGHT).

The tensions on the other leeward mooring cables (B and C) are comparable as they are misaligned with the incoming waves and current. The maximum tensions are measured at mooring line A at water depths of 2 and 5 m (circled in blue) with approximate values of 22 and 50 N, respectively.

3.2.2 Platform Motion

This section reports the findings of platform responses, in which surge, sway and heave time series have been compared for a 180° wave direction and the two water depths. The response is obtained from the floater-mooring coupled responses from 200 to 1000 seconds by omitting the transient period. According to Figure 15, the platform appears to respond similarly in the surge motion at 2 and 5 m water depth, with corresponding maximum displacements of 0.2 and 0.15 m (circled in red).

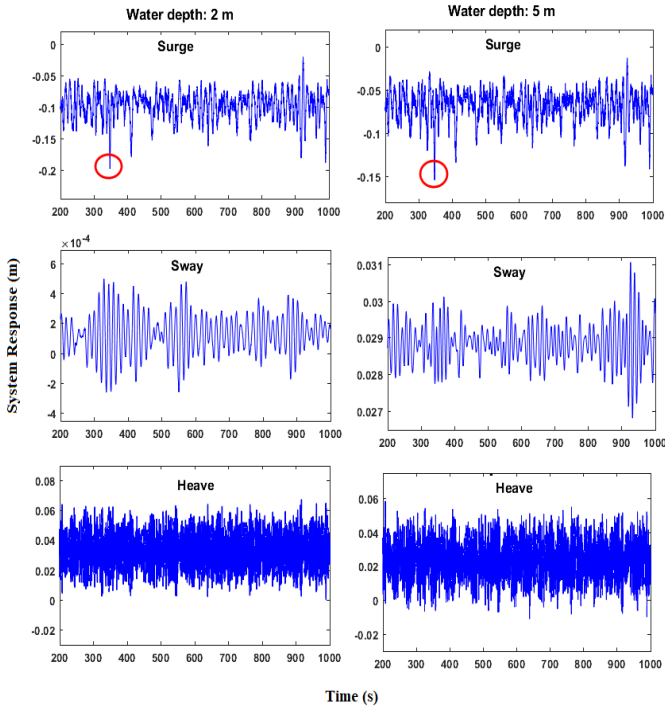


FIGURE 15: TIME-SERIES RESULTS OF THE PLATFORM MOTIONS AT WAVE HEADING 180° AND TWO WATER DEPTHS.

3.2.3 Effect of Wave Directionality

Taking advantage of the platform's capability to weathervane, it is crucial to investigate the consequence of the incoming wave heading on the mooring floater reactions. Thus, a single mooring line's tension and the pitch response are analysed under the most wave-dominated headings in the proposed deployment site, 180° and 210° . As shown in Figure 16, the wave direction does not affect the platform pitch motion.

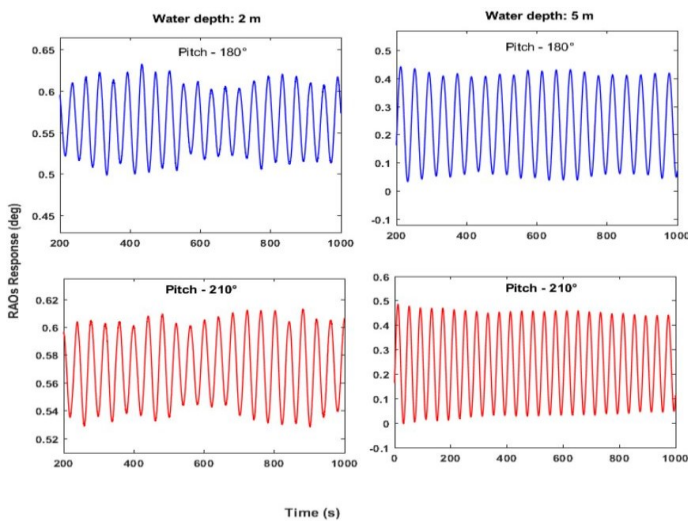


FIGURE 16: TIME-SERIES RESULTS OF THE PITCH RESPONSE AT DIFFERENT WAVE HEADINGS AND WATER DEPTHS.

However, as seen in Figure 17, the wave direction strongly impacts the mooring line tension at both water depths. When a wave with a 180° hits the platform, it tends to severely drift the floater from its initial position, aided by currents from the same direction. On the other hand, when waves attack the platform at a 210° , they lack that significant drift force due to the mooring lines being out of phase with both current and waves, which is clearly seen in the figure.

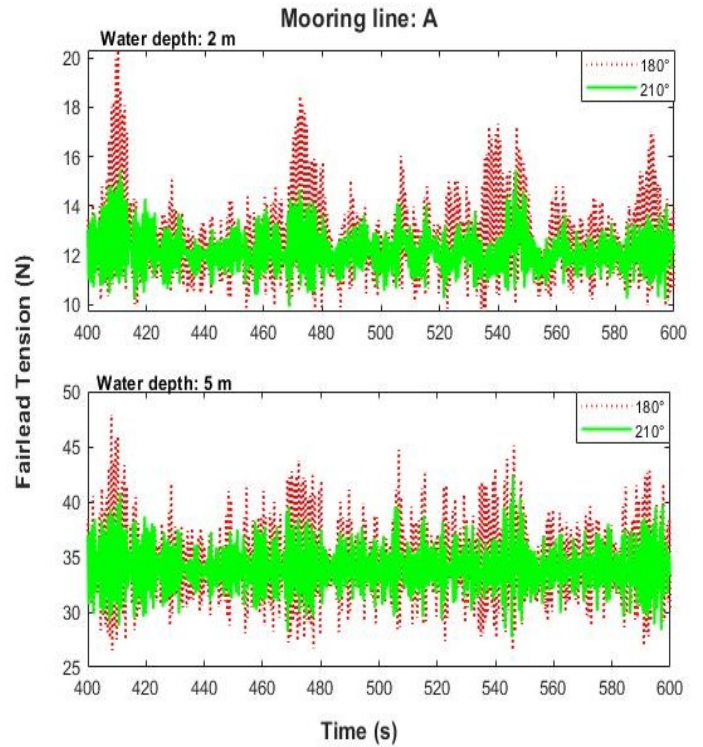


FIGURE 17: TIME-SERIES RESULTS OF A MOORING LINE AT TWO WAVE HEADINGS AND TWO WATER DEPTHS.

3.2.4 Sensitivity of Drag Coefficients

To demonstrate the influence of drag coefficients on the study, the numerical simulations were performed using pontoons of drag coefficients ranging from 0.70 to 1.05; the results reveal that the numerical simulations are insensitive to pontoons C_d values, as illustrated in Figure 18.

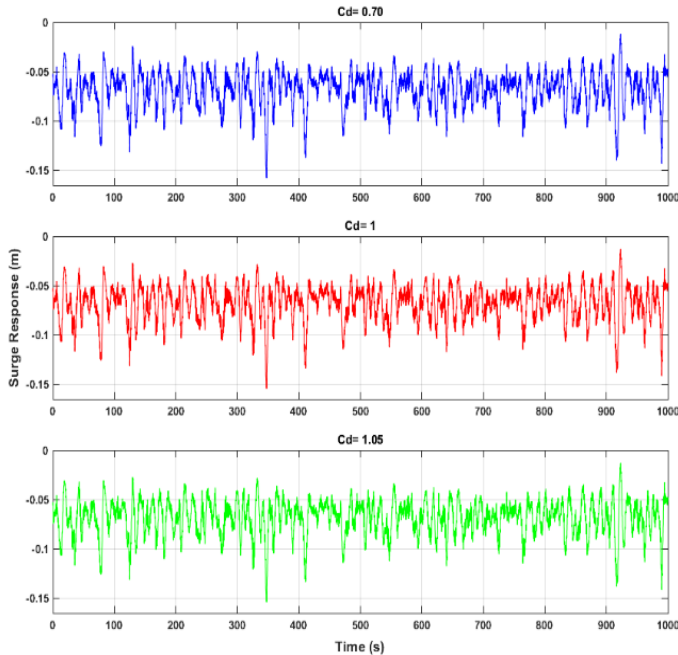


FIGURE 18: TIME-SERIES RESULTS OF THE PLATFORM SURGE MOTION WITH PONTOONS OF DIFFERENT CD VALUES, WAVE HEADING 180° AND WATER DEPTH 5 M.

4 CONCLUSION

The purpose of this study was to assess the hydrodynamic performance for a 1:40 scale model of the W2Power twin-turbine floating platform. Investigations were conducted under survival and operating conditions considering long-term hindcast marine data. Two scaled mooring systems were proposed for moderated and deep waters of depths of 2 and 5 m, respectively.

Eigenfrequency analysis has been carried out; accordingly, the natural periods of floater motions in both heave and pitch have been calculated in detail and presented. The pitch response increased with decreasing water depth, especially at low frequencies, so for a more accurate coupling analysis, it is necessary to obtain the platform's hydrodynamic characteristics for each water depth separately.

In extreme analysis, the significant wave height (H_s) and peak period (T_p) affect both the maximum line tension and platform surge, such that increasing the significant wave height and peak period tends to increase the maximum tension and surge.

The mooring system performs effectively at a water depth of 2 m without requiring as much tension as at a water depth of 5 m, which is a vital sign that the degree of tightness of the smaller water depth is accurately approximated.

The numerical simulations were found to be insensitive to the pontoons' drag coefficient values. The mooring system was found to be sensitive to wave direction, particularly when wave and current directions coincide, even though the aerodynamic loads were not considered. This indicates that waves and current loading and their interaction are crucial in simulations of FOWTs, particularly when the FOWTs are to be deployed in

locations where currents may travel in the opposite direction of the surface wave directions.

Since the platform weathervanes in response to both applied current and wind direction, further work is needed to investigate the impact on either platform stability or power production. Also, future work will explore the wave-current interaction using tank testing experiments in the FloWave Ocean Energy Research Facility to provide validation data for the present simulations and the aerodynamic loads that will be incorporated.

ACKNOWLEDGEMENTS

The authors would like to express their gratitude for funding from the EPSRC and NERC for the Industrial CDT in Offshore Renewable Energy (EP/S023933/1). We are also grateful to Prof. George Kallos and Dr. Christina Kalogeri of the National and Kapodistrian University of Athens for providing the site's hindcast data.

REFERENCES

- [1] The European Parliament and the Council of the European Union, "Offshore Wind Energy in Europe," Brussels, Belgium. pp. 1–6, October 2020: (www.europarl.europa.eu).
- [2] Wind Energy Newsletter, Illustrated by Josh Bauer, NREL, April 2020: (www.nrel.gov).
- [3] N. Barltrop, "Multiple unit floating offshore wind farm (MUFOW)," *Wind Eng.*, vol. 17, no. 4, pp. 183–188, 1993.
- [4] Dagfinn Røyseth, Reza Hezari, Jan Erik Hanssen, W2Power: Combining wind and waves, Proc. 2009 All-Energy Conference & Exhibition, Aberdeen, Scotland, 17 May 2009.
- [5] S. Bashetty and S. Ozcelik, "Design and Stability Analysis of an Offshore Floating Multi-Turbine Platform," in 2020 IEEE Green Technologies Conference (GreenTech), 2020, pp. 184–189.
- [6] H. K. Jang, S. Park, M. H. Kim, K. H. Kim, and K. Hong, "Effects of heave plates on the global performance of a multi-unit floating offshore wind turbine," *Renew. Energy*, vol. 134, pp. 526–537, 2019.
- [7] A. Henderson and M. Patel, "Floating Offshore Wind Farms – an Option?", 2000.
- [8] I. E. Udoh and J. Zou, "Optimizing Floating Offshore Multi-Wind-Turbine Design: A Parametric Study on Tower Inclination and Column Spacing," pp. 1–19, 2020.
- [9] The MARINA Platform project (Jan. 2010 - Jun. 2014), full title Marine Renewable Integration Application Platform, public site: (www.marina-platform.info).
- [10] N. Papandroulakis, C. Thomsen, K. Mintenbeck, P. Mayorga, and J. J. Hernández-Brito, The EU-Project "TROPOS", in *Aquaculture Perspective of Multi-Use Sites in the Open Ocean: The Untapped Potential for Marine Resources in the Anthropocene*, B. H. Buck and R. Langan, Eds. Cham, Switzerland: Springer International Publishing, 2017, pp. 355–374.

- [11] J. E. Hanssen et al., “Design and performance validation of a hybrid offshore renewable energy platform: A path to cost-efficient development of deepwater marine energy resources,” the 10th Int. Conf. Ecol. Veh. Renew. Energies, EVER 2015, 2015.
- [12] M. J. Legaz, D. Coronil, P. Mayorga, and J. Fernández, “STUDY OF A HYBRID RENEWABLE ENERGY PLATFORM: W2POWER,” in the ASME - the 37th International Conference on Ocean, Offshore and Arctic Engineering OMAE2018, 2018, pp. 1–9.
- [13] J. Parfitt, “SPAIN’S FIRST TWO-HEADED FLOATING WIND TURBINE EXPECTED TO BECOME ‘LOWEST COST SOLUTION’ FOR RENEWABLE ENERGY FAR FROM COASTLINE”, The Olive Press, 2019: ([The OLIVE PRESS](#)).
- [14] J. E. Hanssen, Consultation response from 1-Tech SPRL, Brussels (Belgium) - DemoWind Cost modelling: ‘Costing and economic performance of the W2Power floating wind energy technology’, 2019: ([Demo Wind Cost Modelling Report](#)).
- [15] NEWMAN and J.N., “Second-Order, Slowly-Varying Forces on Vessels in Irregular Waves.,” no. 1, pp. 1–4, 1974.
- [16] SESAM-GeniE by DNV, 2021: ([www.dnv.com](#)).
- [17] Orcina Ltd., OrcaWave User Manual, (version 11.a), 2021: ([www.orcina.com](#)).
- [18] Orcina Ltd., OrcaFlex User Manual, (version 11.a), 2021: ([www.orcina.com](#)).
- [19] Atmospheric Modeling and Weather Forecasting Group (AM&WFG), National & Kapodistrian University of Athens, Athens, Greece, 2021: ([www.forecast.uoa.gr](#)).
- [20] Global Wind Atlas: ([www.globalwindatlas.info](#)), accessed in October 2021.
- [21] A. Robertson, J. Jonkman, M. Masciola, and H. Song, “Definition of the Semisubmersible Floating System for Phase II of OC4,” 2014.
- [22] DNV-RP-C205: Environmental Conditions and Environmental Loads - Recommended Practice.
- [23] DNV-OS-E301: Position Mooring.
- [24] A. F. Haselsteiner, J. Lehmkuhl, T. Pape, K. L. Windmeier, and K. D. Thoben, “ViroCon: A software to compute multivariate extremes using the environmental contour method,” SoftwareX, vol. 9, pp. 95–101, 2019.
- [25] M. Hann, D. Greaves, and A. Raby, “Snatch loading of a single taut moored floating wave energy converter due to focussed wave groups,” Ocean Eng., vol. 96, pp. 258–271, 2015.
- [26] R. G. Coe, V. S. Neary, M. J. Lawson, Y. Yu, and J. Weber, Extreme Conditions Modeling Workshop Report, no. July. 2014.